JOURNAL OF CHEMICAL INFORMATION AND MODELING

Article

pubs.acs.org/jcim

Regulation of JAK2 Activation by Janus Homology 2: Evidence from Molecular Dynamics Simulations

Shunzhou Wan[†] and Peter V. Coveney*[,†]

[†]Centre for Computational Science, Department of Chemistry, University College London, London WC1H 0AJ, U.K.

ABSTRACT: Janus kinase 2 (JAK2) is a protein tyrosine kinase implicated in signaling by specific members of the cytokine receptor family. Although it has been established that the JAK2 tyrosine kinase is negatively regulated by the JAK homology 2 (JH2) pseudokinase domain, the underlying mechanism of JH2 mediated regulation remains elusive. To elucidate the regulation of JAK2 kinase, we have built a structural model for the kinase and pseudokinase domains of JAK2. An asymmetric dimer is proposed, in which the kinase domain JH1 occupies a position where it could not be activated. We investigate the dynamic and energetic properties of the dimer by molecular dynamics simulation. JAK2 activation requires the two domains to be dissociated and rearranged in a form such that the JH1 kinase domain can adopt an active conformation. The significance of the above mechanism is emphasized by the finding that the activating V617F mutation destabilizes JH1−JH2 association in the proposed asymmetric dimer. Thus abrogation of the domain−domain interaction seems to be a possible first step for the structural rearrangement of the two domains, resulting in constitutive activation of JAK2 by the V617F mutation.

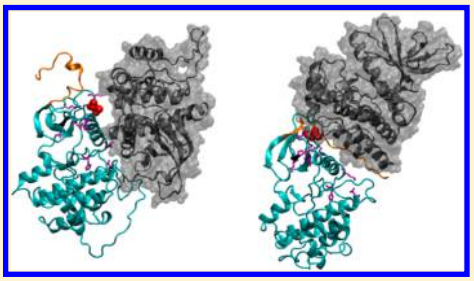

INTRODUCTION

JAK2, a member of the Janus kinase (JAK) family of nonreceptor tyrosine kinases, participates in the evolutionarily conserved JAK/STAT signaling pathway in almost all eukaryotic organisms.[1] The kinase was named after the mythical two-faced Roman god, Janus, which portrays similar structural and functional characteristics: it consists of a kinase and a pseudokinase domain and possesses but also negatively regulates the kinase activity. There are four principal components in the JAK/STAT pathway:[2] i) cytokines and cytokine receptors, of which the binding initiates a transduction signal, ii) members of the JAK family which are then activated and autophosphorylated, iii) STAT (signal transducer and activator of transcription) proteins which are subsequently phosphorylated and translocated to the nucleus, and iv) STAT target genes whose transcriptional activation is facilitated. The pathway regulates numerous aspects of hematopoiesis and the immune response, and its abnormal activation has been implicated in the promotion of cancers[3] and immune disorders.[4] JAK2, like many other members of the protein kinase superfamily,[5] has become a potential drug target for treatment of a number of diseases.

JAK2's importance is further underscored by its constitutive activation (i.e., it is always turned on) via cancer mutations, which contributes to its pro-proliferation activities. JAK2 has seven defined regions called Janus homology domains 1−7 (JH1−7). JH1 and JH2 are homologous phosphate-transferring domains; JH1 exhibits tyrosine kinase catalytic activity, while JH2 is a pseudokinase domain essential for regulation of tyrosine phosphorylation[6] but itself lacking enzymatic activity; the SH2-like (JH3) and FERM (band 4.1, ezrin, radixin, and moesin, JH4−7) domains are involved in JAK2 interactions with other molecules. The existence of pseudokinases is not an unusual biological phenomenon; it has been estimated that up to 10% of the kinome could be comprised of pseudokinases as they appear to lack key residues required for catalysis.[7] The JH2 domain, along with many other pseudokinases,[7] has been proven to act as allosteric regulator of other protein kinase domains. In experiments, removing JH2 leads to constitutive activity of JH1 in the absence of upstream signaling.[6] Most JAK2 mutations are found in the JH2 domain and the connecting region between JH2 and JH3 domains (Figure 1);[8] the most common mutation is V617F in JH2, which occurs frequently in two types of blood disorders −75% of essential thrombocythemia (ET) and 97% of polycythemia vera (PV).[9]

Many studies have sought to understand kinase signaling pathways and their role in various diseases. The analyses of sequences, structures, function, and the interactome of protein kinases have all provided important foundations to gain further insight into the mechanism of kinase activation and to design targeted kinase inhibitors.[10] Among the 518 known members of the kinase superfamily, some are widely documented in numerous studies, while others have hitherto not been well-explored. Epidermal growth factor receptor (EGFR) is one of the former; it has been identified as an important molecular marker with prognostic and therapeutic significance in lung carcinogenesis. JAK2 is one of the less-explored members, at least from the structural point of view. The X-ray structures of the JAK2 kinase domain have just begun to emerge in the last four years. There were still no crystallographic structures for the JH2 regulatory domain when our simulations were performed, not to mention the whole JAK2 protein. Three X-ray structures were recently reported for both wild-type and V617F mutant

Received: July 4, 2012
Published: October 4, 2012

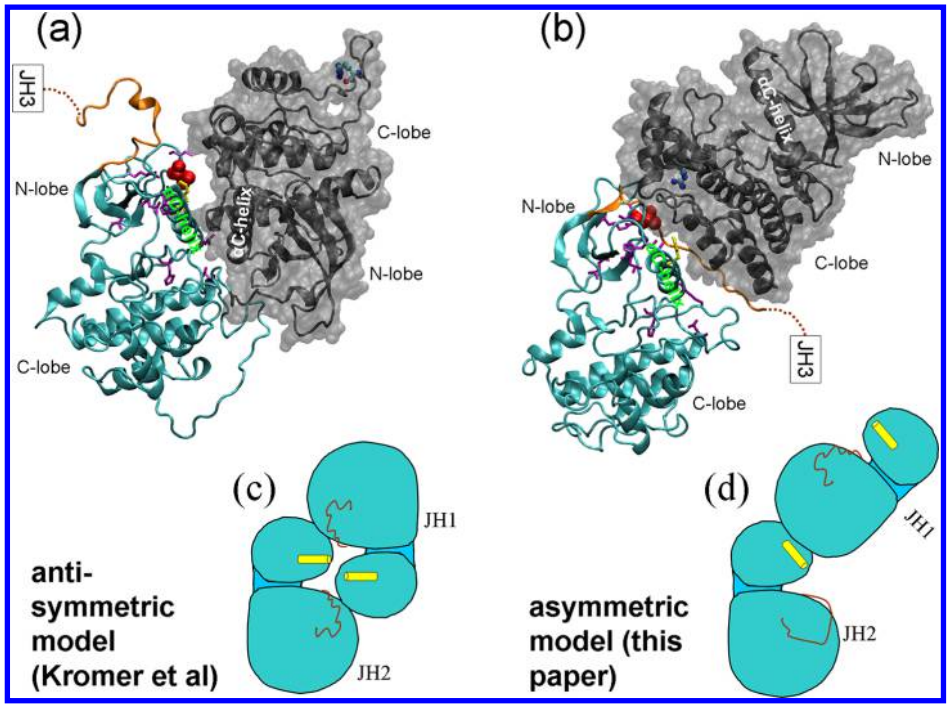

Figure 1. The structures of the JH1−JH2 dimer in antisymmetric (a,c) and asymmetric (b,d) modes. The proteins are shown in cartoon representation (a,b), with JH1 in gray and JH2 in cyan. JH1 is also shown in surface representation for better visualization of the interacting surface between the two domains. The V617F mutation in JH2 is shown in a ball and stick model (red), F595 in bond (yellow), R1063 in JH1 domain in ball and stick (cyan for carbon, blue for nitrogen, and red for oxygen), other JH2 mutations in bond (purple), and the link between JH2 and JH3 in cartoon representation (orange). The antisymmetric structure (a) is constructed based on coordinates of a previously built model,[12] while the asymmetric model (b) is based on an EGFR homodimer (PDB id: 1M14).[30] The structure of JH1 was taken from X-ray coordinates (PDB id: 3E64),[31] while JH2 is built using a homology modeling method based on the same EGFR X-ray structure.[30] The schematic representations (c,d) highlight the distinct arrangements of the two domains and the conformational differences of the αC-helix (yellow) and A-loop (orange) within the JH2 domain.

JH2 domain,[11] which will be addressed in the following analyses and discussion.

Structures of JH1−JH2 domains[12] and all seven homology domains[13] of JAK2 were constructed a decade ago using homology modeling techniques, based on limited crystallographic and genetic data available at that time ("Kromer's model", see Figure 1a,c). In Kromer's model, the JH1 and JH2 domains form an antisymmetric dimer in which the N- and C-lobes of JH1 contact the C- and N-lobes of JH2, respectively. The term "dimer" as used hereafter refers to a complex formed by two kinase(-like) domains, regardless of whether they are from the same JAK2 molecule or not. The JAK2 dimer reported in the literature,[14] on the other hand, usually means a complex of two full-length JAK2 molecules. The JH1-JH2 structure was constructed based on a proposed dimeric form of fibroblast growth factor receptor (FGFR).[15] The catalytic activities and mutational effects were interpreted in terms of the interactions of JH2 on the kinase domain JH1, which affect the conformation of the A-loop and αC-helix in the JH1 domain.[12,16−18] Since then further studies have been carried out on JAK2, and protein kinases in general, to understand their kinase functions and regulations. The number of kinase structures deposited in the Protein Data Bank (PDB) has been increasing rapidly in recent years. There were only 202 structures related to protein kinases before 2001 when the JAK2 structure[12] was constructed; 2570 structures have been added since then, including all 22 JAK2-related structures (as of 30 April 2012). In addition to the structures of the single kinase domain, allosteric regulation of protein kinases is also well studied, including dimerization of protein kinases alongside interactions between kinases and other proteins.[19] The antisymmetric mode (Figure 1a,c) has not been reported in any pairs of protein kinase domains.

An asymmetric head-to-tail dimerization (Figure 1b,d) has been established for EGFR, based on experimental study of point mutations at the interface.[20] Indeed the asymmetric form is one of three suggested FGFR dimerizations in the exact study[15] the Kromer's model was based on and is the one verified later by structural and biochemical experiments.[21] In our mode, the N-lobe of one kinase domain (monomer A) makes contact with the C-lobe of the other kinase domain (monomer B). The monomer B, termed the "activator", acts as an allosteric modulator by inducing and stabilizing the monomer A, termed the "receiver", in a catalytically active conformation characterized by the orientation of the αC-helix and the extended conformation of the A-loop (Figure 1d). Intradomain interactions affect the orientation and position of the receiver's αC-helix, which in turn change the conformation of the activation loop.[20] Kinase assays have shown that blockage of EGFR dimerization, by mutating residues at the dimer interface[20] or by binding other molecules at the asymmetric dimer interface,[22] can extinguish its kinase activity. The asymmetric dimer has been directly visualized in a negative-stain electron microscopy experiment.[23] Although it coexists in both symmetric dimer (two domains are related by a 2-fold axis, and make contact with their N-lobes) and monomer states, the formation of the asymmetric dimer exhibits elevated catalytic activity.[23] The formation of an asymmetric dimer is

dx.doi.org/10.1021/ci300308g | J. Chem. Inf. Model. 2012, 52, 2992−3000

not limited to homodimers of two EGFRs. The same association has been found between two different members of the ErbB family,[23,24] various tyrosine kinase domains such as those of the FGFR,[21] and other members of the protein kinase superfamily such as the cyclin-dependent kinase (CDK)/cyclin complex[25] and histidine kinase.[26] Indeed, the asymmetric dimer has been suggested as a general model for other kinases.[20,27] The probability of a protein kinase acting as an "activator" or a "receiver" varies depending on the specific protein. ErbB3, a pseudokinase member of the ErbB family, is suggested to serve as an activator of other ErbB family members.[24] Imaging experiments have also shown that EGF-stimulated EGFR prefers to adopt the receiver position in the asymmetric EGFR/ErbB2 heterodimer.[28]

JH2-based regulation of JAK2 may rely on interactions similar to those found in these asymmetric dimers. One possible mechanism is that regulation is achieved by JH2 occupying the receiver position in the JH1−JH2 dimer, which keeps JAK2 in its inactive state; JAK2 activation requires the JH1 domain to act as the receiver in the JH1−JH2 or JH1−JH1 dimer, adopting a conformation essential for catalysis. In this study, we investigate JH2-mediated regulation by molecular modeling of an asymmetric JH1−JH2 dimer in which JH2 is located at the receiver position.

METHODS

Preparation of Modeling Systems. The structure of the JAK2 JH2 domain was constructed using MODELLER,[29] a homology modeling software tool for predicting the three-dimensional structures of proteins. The X-ray structure of EGFR (PDB id: 1M14)[30] was used as the template structure. The kinase domains of JAK2 and EGFR have ∼21% sequence identity and another ∼41% similarity. The highly homologous catalytic kinase core predominates the high degree of structural conservation for JAK2 and EGFR. The conserved residues mainly line the active site and the secondary structures, while many of them interact with adenosine triphosphate (ATP) substrate. The homology model of the JH2 domain closely resembles most X-ray structures of tyrosine kinase domains but displays a different conformation from the JH2 X-ray structure in a region including the A-loop and another loop between β-strand 7 (β7) and β8.[11] This region does not contact JH1 directly in our model and is not expected to affect the JH1-JH2 interaction significantly in the asymmetric conformation. The structure of the JH1−JH2 dimer was constructed based on the same EGFR structure, in which the JH1 coordinates were taken from an X-ray structure (PDB id: 3E64).[31] In the dimer, JH1 was located as the activator and JH2 as the receiver. Choosing the same EGFR structure as template for both the JH2 and JH1−JH2 structures may make the JH1−JH2 interface less sterically hindered. The V617F mutant JH2 was obtained by modification of valine at 617 to phenylalanine within the JH2 structure. Four molecular models were constructed for WT and V617F mutant JAK2 systems which are designated as WT-JH2, V617F-JH2, JH1-WT-JH2, and JH1-V617F-JH2, respectively. The modeled structures are available on request (e-mail: p.v.coveney@ucl.ac.uk).

Initial preparation of all four models was implemented using the Binding Affinity Calculator.[32] Protonation states were assigned for all ionizable residues to their default values at neutral pH. The proteins were solvated using TIP3P water molecules[33] and then electrostatically neutralized by adding counterions (Na^+). The distance between the edges of the solvent box and the closest atom in the protein was 14 Å. The AMBER ff03 all-atom force field[34] was used to describe the protein parameters. This procedure resulted in a final atom count of approximately 52,000 and 96,000 atoms for the JH2 domain and JH1−JH2 domain models respectively.

Simulation. Molecular dynamics (MD) simulations were performed on the four separate JAK2 models that differ in terms of sequence (wild-type or V617F mutation) or size (JH2 domain alone or JH1−JH2 domains). The MD package NAMD2.7[35] was used throughout the equilibration and production simulations. For each molecular system, energy minimizations were first performed with heavy protein atoms restrained at their initial positions. Then a series of short simulations (each of 25 ps duration) were conducted, while the restraints on heavy atoms were gradually reduced. Finally, 100 ns production simulations were run, and coordinates were recorded at every 10 ps. Periodic boundary conditions were imposed in all three spatial dimensions. The systems were maintained at a temperature of 300 K and a pressure of 1 bar in the isothermal−isobaric ensemble (NPT). The simulations were performed on 96 cores (four 24-core nodes) for the JH2 system, and 192 (eight 24-core nodes) for JH1−JH2, on HECToR (Cray XE6), the UK national supercomputer based in Edinburgh (http://www.hector.ac.uk/). Each individual MD simulation took approximately 2 h/ns on HECToR.

Analyses. Analysis of the root-mean-square deviation (RMSD) was conducted for the backbone atoms, based on comparison with the initial structures. Thermodynamic analysis was performed using the molecular mechanics Poisson−Boltzmann surface area (MM/PBSA) method[36] within the AMBER package.[37] The MM/PBSA method is an efficient way to estimate the binding free energy of a complex from a classical MD simulation. The JH1−JH2 binding free energy can be evaluated, following the MM/PBSA approach, as

$$\Delta G_{binding} = G^{dimer} - G^{JH1} - G^{JH2} \tag{1}$$

where

$$G^{i} = \langle E_{MM} \rangle + \langle G_{solv} \rangle - TS_{conf} \tag{2}$$

Here, $\langle ... \rangle$ denotes an average for a set of structures from MD simulations, while E_{MM} is the molecular mechanics energy of species i (the index i corresponding to either dimer, JH1 or JH2 domain) in the gas phase. E_{MM} is the sum of bonded energy, van der Waals (E_{vdW}), and electrostatic (E_{elec}) interactions. G_{solv} is the solvation free energy; it is estimated as the sum of the electrostatic solvation free energy (G_{PB}) calculated using the Poisson−Boltzmann equation and the nonpolar solvation free energy (G_{SA}) calculated from the solvent accessible surface area. $-TS_{conf}$ is the contribution from the configurational entropy S_{conf} at temperature T. As the JH1 and JH2 domains bind noncovalently, the bonded terms cancel exactly in the binding free energy calculation (eq 1). Hence, the binding free energy can be written as

$$\begin{aligned} \Delta G_{binding} &= \langle \Delta E_{MM} \rangle + \langle \Delta G_{solv} \rangle - T\langle \Delta S_{conf} \rangle \\ &= \langle \Delta E_{vdW} \rangle + \langle \Delta E_{elec} \rangle + \langle \Delta G_{PB} \rangle + \langle \Delta G_{SA} \rangle \\ &\quad - T\langle \Delta S_{conf} \rangle \end{aligned} \tag{3}$$

Here, the free energy difference upon binding $\Delta G_{binding}$ is decomposed into ΔE_{MM} and ΔG_{solv} and further into ΔE_{vdW}, ΔE_{elec}, ΔG_{PB}, and ΔG_{SA}. The $-T\Delta S_{conf}$ term denotes the

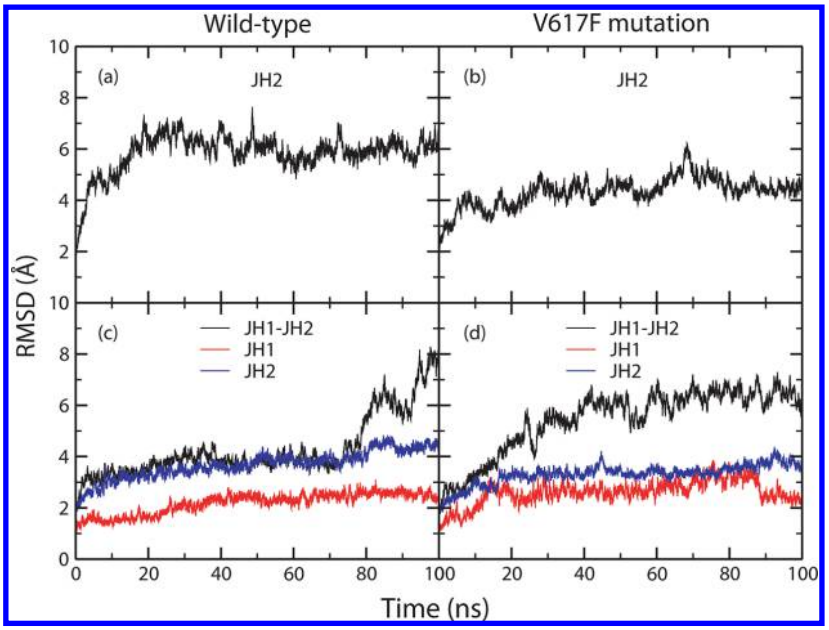

Figure 2. Root-mean-square deviation (RMSD) as function of MD simulation time for the backbone atoms, with respect to the initial structures for (a) wild-type JH2, (b) V617F mutant JH2, (c) wild-type JH1−JH2, and (d) V617F mutant JH1−JH2. The JH2 domain displays a large deviation from the initial structures as shown in (a) and (b). The RMSD increases of the JH1−JH2 dimer in (c) and (d) indicate relative domain movement, possibly evidence of their incipient separation.

configurational entropy change ΔS_{conf} at temperature T. The entropy contribution ΔS_{conf} was not included in this study. Previous study has shown that inclusion of the configurational entropy does not make any significant contributions to estimation of protein stability for the Abelson and EGFR kinases.[38] The structures used for the thermodynamic calculations were extracted from the last 80 ns MD trajectories of the JH1−JH2 systems.

RESULTS

Locations of Cancer-Related Mutations. Negative-stain electron microscopy experiments have demonstrated that a mutation at the asymmetric interface eliminates the association of the dimeric EGFRs and hence suppresses EGFR kinase catalytic activity.[23] For the regulation-related mutations in the JH2 domain of JAK2, it is reasonable to assume that most are located at or near the JH1−JH2 interface. The mutations either strengthen or weaken the interactions between JH1 and JH2 domains and hence affect regulation of the JAK2 kinase activation.

From a visual inspection of the asymmetric JH1−JH2 structure constructed here and the previously built antisymmetric model,[12] it is apparent that the mutations are in closer proximity to the interface in the asymmetric dimer than they are in the antisymmetric form (Figure 1). For example, V617, the more commonly mutated residue of JAK2, is closer to the kinase domain JH1 in the asymmetric model than it is in the antisymmetric one, with closest heavy atom distances of 3.2 Å and 7.9 Å in the two models. Mutations are present at the link region between JH2 and JH3 in patients with myeloproliferative neoplasm and polycythemia vera.[39] This region has a close contact with the JH1 domain in the asymmetric model, but no direct interactions with JH1 in the antisymmetric model (Figure 1). R1063H, a mutation in JH1 domain identified in some polycythemia vera patients, is also near the JH1-JH2 interface in the asymmetric model with a closest distance of 4.7 Å to the JH2 domain, while the residue is far away from the interface in the antisymmetric conformation with a distance of 34.0 Å.

Initial Separation of the Two Domains in the V617F Mutant JAK2. Figure 2 shows the root-mean-squared deviation (RMSD) of backbone atoms for JH2 and JH1−JH2 domains, with respect to the structures from which the simulations are initiated. The simulations of JH2 alone were initiated from a structure built by homology modeling. It is not surprising that its RMSD displays a rapid increase in the first 20 ns simulation, both for the wild-type and V617F mutant forms (Figure 2a,b) because of the uncertainties in the modeled structures.[40] The V617F mutant JH2 has a smaller RMSD than the wild-type after 20 ns simulations, probably due, at least in part, to the presence of F617 which stabilizes the αC-helix in the N-lobe.[11] The interactions between JH1 and JH2 stabilize the N-lobe of the JH2 (Figure 1) and are attributed to the decreased JH2 flexibility. The wild-type simulation of JH1−JH2 displays RMSD values of ca. 4 Å for the whole dimer after approximately 20 ns and remains as such for about 55 ns when the value begins to increase. As the RMSDs for the JH1 or JH2 domain alone remain stable throughout the last 80 ns simulations, the rapid increase of the RMSD for JH1−JH2 is due to the relative movement between the two domains, possibly implicating incipient JH1−JH2 separation. The V617F simulation, by contrast, does not exhibit any stable period before it reaches equilibrium at about 40 ns, with a much larger RMSD than that of the wild-type at its stable state. Although the wild-type and mutant JH1-JH2 have comparable RMSD during the last 20 ns of the simulations, they adopt different orientations of JH1 and JH2. At the end of the simulations, for example, the two structures differ by an RMSD larger than 7.5 Å for all backbone atoms, mainly due to the differences in the interdomain orientations. The mutation is likely to make the JH1−JH2 structure unstable and possibly contributes to the separation of JH1 and JH2 from the asymmetric mode at an

dx.doi.org/10.1021/ci300308g | J. Chem. Inf. Model. 2012, 52, 2992−3000

earlier stage, within the first 40 ns simulation (Figure 2d), than that in the wild-type dimer (Figure 2c).

The relative location of the JH1 and JH2 domains is reflected in the distances between the centers of mass of the two adjacent lobes and their interface plane (Figure 3). The

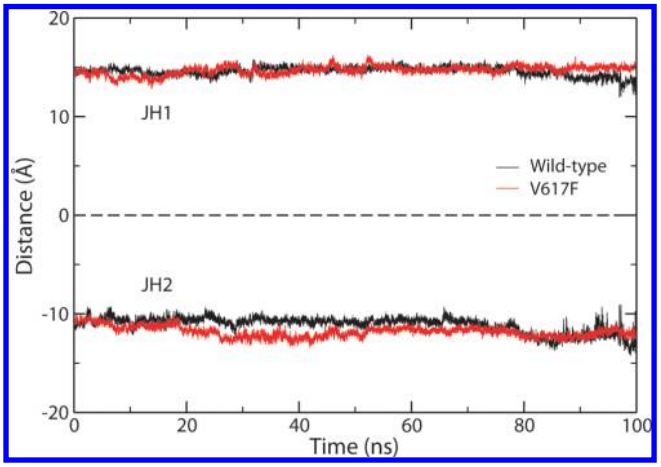

Figure 3. The interface distances of JH1 and JH2. The distances are measured between the center of mass of the C-lobe to the interface plane (dashed line) for the JH1 domain and the center of mass of the N-lobe to the same plane for the JH2 domain. The interface plane is defined by a least-squares-plane through the atoms which belong to the JH1 or the JH2 domain and are within 5 Å from the JH2 or the JH1 domain, respectively.

interface is defined by least-squares fitting of a plane to a set of selected atoms which belong to the JH1 or JH2 domain and are within 5 Å of the JH2 or JH1 domain, respectively. The centers of mass are defined by the C-lobe of the JH1 domain and the N-lobe of the JH2 domain (Figure 1); the other two lobes are not used as the interlobe movement within one domain could introduce large fluctuations of its center of mass. The salient difference of the RMSD (Figure 2) in the whole wild-type and V617F mutant JAK2 is also reflected in the interface distances of the two domains (Figure 3): the mutation makes the JH2 domain move further from the interface within the first 40 ns of the simulation, most likely because of the intrusion of the hydrophobic phenylalanine side chain into a polar environment. The JH2-interface distance shows larger differences between the wild-type and mutant JAK2 than the JH1-interface distance. The C-lobe, consisting of an α-helix bundle, is more stable than the N-lobe which contains a 5-stranded β-sheet and a single α-helix (Figure 1). The mutation within the JH1–JH2 interface is more likely to disrupt the less stable N-lobe of the JH2 domain and indeed may fail to form the stable dimer displayed in Figure 1b.

It should be noted that the dissociation of a protein–protein complex, with k_{off} generally in the order of magnitude of 10^{-3}–10^{-6} s^{-1},[41] takes place on a much longer time scale than that of the simulations reported in this study. It is not surprising that the distances between the two domains are very similar for the wild-type and mutant forms in our 100 ns simulations. Both the wild-type and mutant JH1-JH2 dimers are expected to dissociate from the proposed conformation and to rearrange into a biologically active structure. The V617F mutation is likely to make the dissociation easier by inducing a local conformational change at the interface, whereas the inter-domain interaction is weakened (see energy analyses below) but the distance not significantly altered at the very beginning of the domain separation process. A reduced JH1–JH2 interaction essentially functions as a trigger for the dissociation of the two domains, which must be followed by a series of large-amplitude conformational changes. The local conformational changes and the structural features could be better captured by ensemble simulations[42] with much higher computational effort, while the large scale domain–domain separation process occurs on a time scale that is unreachable by standard molecular dynamics simulations with the computing power available today.

Buried Surface of JH2 Domain. The V617F mutation introduces a large hydrophobic group which is buried at the JH1–JH2 interface (Figure 1b). The interfacial residue F617 has a larger contact surface with the JH1 domain than V617 does (Figure 4). In the modeled asymmetric dimer, the five

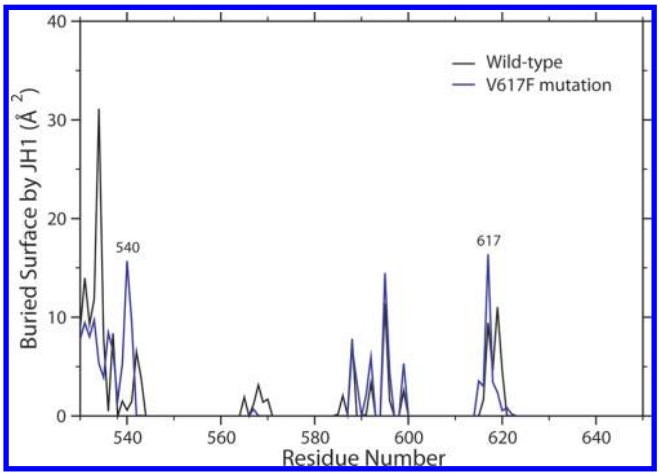

Figure 4. The contact surfaces of JH2 residues buried by the JH1 domain. The substitution of valine by phenylalanine at position 617 introduces a large change in the buried surface area of this residue and also of the link region (residue numbers 530–542) between JH2 and JH3 domains.

closest residues of JH1 to residue V617 are N1084, N1085, R1087, N1107, and N1108; four of them are polar asparagine residues, the last one being a charged arginine. The surface formed by these residues is hydrophilic and disfavors the bulky hydrophobic side chain of phenylalanine. Replacement of valine with such a residue could destabilize the association of the JH1–JH2 dimer and make them separate more easily. The separated JH1 and JH2 would thus be able to rearrange in a form such that JH1 occupies the receiver position and is biologically activated (see further below and Figure 5). We hypothesize that large hydrophobic residues at position 617 would render the kinase domain constitutively active in a manner similar to that described above for the V617F mutation. The hypothesis is supported by an experimental mutagenesis study which identified that only the substitution of bulky hydrophobic residues at position 617 (V617W, V617M, V617I, V617L, and V671F) is able to induce constitutive downstream signaling.[43] The V617I mutation has been reported in patients with hereditary thrombocytosis,[44] while V658L in JAK1, a mutation analogous to V617L in JAK2, has been reported in patients with acute leukemia.[45] V617M and V617W are unlikely to occur as the substitutions require two and three base pair changes in the DNA codon for valine.

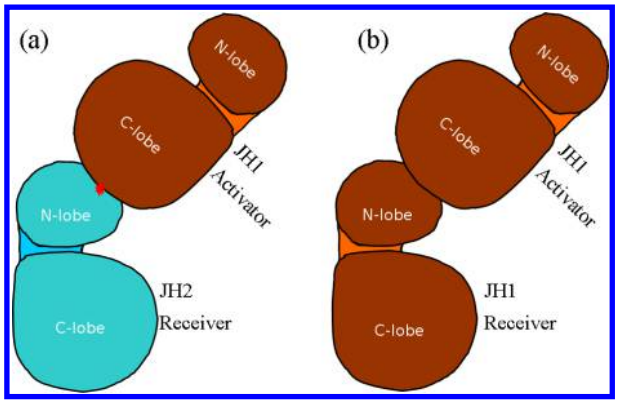

Figure 5. A model for the function of the JH2 domain in activating JAK2. Under normal physiological conditions, JAK2 is autoinhibited through an asymmetric dimer in which JH2 (blue) acts as the receiver and JH1 the activator (orange) (a). Activating mutation (red star) at the dimer interface (a) results in the separation and rearrangement of the kinase domains, possibly forming a JH1 homodimer (b) and leading to the activation of the JH1 domain.

Constitutive activation of V617F mutant JAK2 requires the presence of residue F595.[16] Mutagenesis experiments have shown that the activity of V617F mutant JAK2 decreases significantly when the F595 is replaced by Ala, Val, Ile, or Lys, while the activity is maintained when replaced by aromatic residues Tyr and Trp.[16] While it is proposed from the antisymmetric model[12] that the activity changes are induced by F617 and F595 indirectly through affecting the JH1 conformations,[16] we hypothesize from our model that the residues F617 and F595 play a role mainly through their direct interactions with the JH1 domain. Residues F617 and F595 are in close proximity, and both make contact with the hydrophilic surface of JH1 identified above. The substitutions of F595 with similar bulky and hydrophobic residues (Tyr and Trp) do not change the local interactions significantly; the replacements with small side-chain residues (Ala, Val, Ile) make F617 less sterically hindered and reduce the unfavorable JH1-JH2 interactions; mutation to a charged residue (Lys) introduces a more favorable electrostatic interaction with the hydrophilic surface of JH1, which overwhelms the unfavorable steric interaction induced by its side chain. The changes in the JH1-JH2 interactions caused by F595 substitutions, i.e. more favorable with Lys, less unfavorable with Ala/Val/Ile, and little discernible with Tyr/Trp, are all in line with the relative changes of JAK2 V617F activities measured experimentally.[16]

A variety of JAK2 exon 12 mutations are present in V617F-negative patients with myeloproliferative neoplasm and cythemia vera, of which the most frequently occurring are in the link region between JH2 and JH3 domains (Figure 1).[39] This region is likely to participate in the JH1−JH2 interactions, just as the juxtamembrane region contributes to asymmetric contacts in the EGFR dimer.[48] The contact interface changes substantially with this region upon the V617F mutation (Figure 4). Residue I540 has a much larger buried surface in the mutant JH1−JH2 than that in the wild-type, while most of the other residues in the link region have less buried surfaces. Mutations, deletions, and insertions around I540 have been reported in polycythemeia vera patients, with or without the V617F mutation.[47] One can envision that mutations in this region affect the interactions of JH2 with JH1 and hence the regulation of JH2 on kinase activity.

Binding Free Energy of JH1−JH2. We performed MM/PBSA calculations to get quantitative estimates for the binding free energies and their components. The binding free energies averaged over all conformations sampled in the last 80 ns simulations are listed in Table 1 for the wild-type and mutant JH1−JH2 dimers. Our MM/PBSA calculations show that the binding free energy of wild-type JH1−JH2 is 10.4 kcal/mol more favorable than that of the V617F mutant dimer.

The JH1 domain has very similar free energy in the two simulations (Table 1) as the C-lobe of the JH1 domains is relatively stable and thus hardly affected by mutations in JH2 on the sampled time scale. Direct comparison of the energy components between the two protein systems is not straightforward, because competing effects ($\Delta\Delta G_{PB}$ and $\Delta\Delta E_{elec}$ for example) can be quite different but tend to cancel each other out. Nevertheless, it becomes clear from the energy decomposition (Table 1) that the direct interdomain electrostatic interactions are favorable to the binding for both wild-type and mutant systems, although the energies could not compensate the large desolvation penalties associated with the binding event, thereby leading to an unfavorable total electrostatic contribution. The V617F mutation makes the electrostatic interaction between two domains much weaker ($\Delta\Delta E_{elec}$ = 96.5 kcal/mol), which cannot be fully compensated by the smaller solvation penalty ($\Delta\Delta G_{PB}$ = −82.3 kcal/mol). The more favorable binding free energy of the wild-type JH1−JH2 is due to its less unfavorable total electrostatic interactions compared with the V617F mutant. This finding is not unexpected as the residue 617 interacts with a polar/charged region of JH1; the intrusion of a large hydrophobic group should indeed be energetically unfavorable.

Asymmetric vs Antisymmetric Models. Two different molecular mechanisms are behind the proposed dimeric forms of the kinase(-like) domains of JAK2 for its activation and regulation. In the antisymmetric conformation,[12,16−18] the A-loop and αC-helix of kinase domain JH1 directly interact with the pseudokinase JH2 domain (Figure 1a,c). Regulation is achieved by restricting the A-loop in a closed conformation, while maintaining the JH1 domain in an inactive conformation. Mutations change the interdomain interactions, causing the A-loop of JH1 to become extended and hence the active site is highly accessible.[17]

In the asymmetric model, one domain acts as a receiver, while the other acts as an activator.[28] The receiver can adopt a structurally active conformation with specific A-loop conformation and αC-helix orientation (Figure 1d), although JAK2 may still remain in a catalytically inactive state when the JH2 domain acts as the receiver. In this model, the αC-helix but not the A-loop of the receiver interacts with the other domain directly. The interdomain interaction rotates the αC-helix to the active state which then promotes the conformational switch of the A-loop from an inactive packed position to an active extended, more open form (Figure 1d). The activation and regulation of JAK2 are determined by how well the JH1 domain occupies the receiver position. Although both JH1 and JH2 can act as the receiver, under most physiological conditions the JH2 domain is believed to adopt this position, putting JAK2 into a catalytically inactive state. Mutations in the JH2 domain weaken the JH1-JH2 interaction, making JH1 more likely to adopt the receiver position.

Specific mutations in the proposed dimer interfaces should enable us to verify the interdomain arrangement, as was done for EGFR.[20] However, mutations within the C-lobe of the JH1

Table 1. JH1−JH2 Interactions (kcal/mol) Calculated Using the MM/PBSA Method

	wild-type				V617F				
type[a]	complex	JH1	JH2	Δ^b	complex	JH1	JH2	Δ^b	$\Delta\Delta^c$
E_{vdW}	−4857.5 (0.5)	−2466.7 (0.5)	−2291.7 (0.3)	−99.1 (0.1)	−4817.4 (0.3)	−2430.1 (0.2)	−2284.6 (0.3)	−102.6 (0.2)	−3.5 (0.2)
E_{elec}	−40544.6 (4.3)	−20531.4 (2.7)	−19826.4 (3.1)	−186.9 (0.8)	−40171.8 (2.7)	−20427.8 (2.3)	−19653.6 (1.9)	−90.4 (0.7)	96.5 (1.1)
G_{PB}	−6801.0 (3.9)	−3310.7 (2.5)	−3730.7 (2.9))	240.4 (0.7)	−7144.6 (2.5)	−3456.8 (2.2)	−3845.9 (1.5)	158.1 (0.7)	−82.3 (1.0)
G_{SA}	150.7 (0.1)	79.1 (0.0)	82.3 (0.0)	−10.8 (0.0)	158.3 (0.0)	84.1 (0.0)	85.2 (0.0)	−11.0 (0.0)	−0.2 (0.0)
E_{MM}	−45402.1 (4.7)	−22998.1 (3.0)	−22118.1 (3.3)	−286.0 (0.8)	−44989.2 (2.8)	−22857.9 (2.3)	−21938.2 (1.9)	−193.0 (0.6)	93.0 (1.0)
G_{solv}	−6650.2 (3.8)	−3231.5 (2.5)	−3648.4 (2.9)	229.6 (0.7)	−6986.3 (2.5)	−3372.7 (2.2)	−3760.8 (1.5)	147.2 (0.7)	−82.4 (1.0)
total	−52052.4 (1.3)	−26229.6 (0.9)	−25766.4 (0.7)	−56.3 (0.2)	−51975.5 (0.8)	−26230.6 (0.4)	−25699.0 (0.6)	−45.9 (0.2)	10.4 (0.3)

[a]See eq 3. [b]$\Delta = E_{Complex} - E_{JH1} - E_{JH2}$. [c]$\Delta\Delta = \Delta_{V617F} - \Delta_{Wild\text{-}type}$. The uncertainties were estimated from the block average method,[52] with block size of 1 ns.

domain may also affect its preference to form an active conformation, as JH1 may involve the same residues to contact the other unit in both the active and inactive forms (Figure 5). Other experimental methods, including luciferase fragment complementation imaging,[28] negative-stain electron microscopy,[23] and X-ray crystallography, would be able to provide direct evidence for the dimerization of the kinase(-like) domains of JAK2 and other protein kinase domains.

DISCUSSION

The kinase regulation of JAK2 has been proven to rely on interaction between the two JAK homology domains JH1 and JH2,[48] which maintains JH1 in an inactive conformation. In this study, a molecular mechanism has been investigated for this regulation caused by an asymmetric dimerization of JH1 and JH2 domains, and the mutational effects analyzed with respect to the association of the JH1−JH2 dimer. We have built an asymmetric dimer of JH1 and JH2 domains, and used molecular dynamics simulations to study the JH1−JH2 interactions responsible for the negative regulation of JH2 on JAK2 activation.

This asymmetric dimer exhibits interactions reminiscent of those found in members of the ErbB family and other protein kinases. The EGFR/ErbB2 heterodimer consists of a specific arrangement after EGF stimulation, in which EGFR adopts the receiver position in the asymmetric dimer and is activated first.[28] EGFR activation is followed by separation of the EGFR/ErbB2 dimer and reformation of the dimer with ErbB2 now in the receiver position. This mechanism, and the corresponding structural arrangement of EGFR/ErbB2, are likely to be utilized by other ErbB dimers[28] and possibly by other kinases. We hypothesize here that, under normal physiological conditions, JAK2s are brought together in an unproductive configuration. Their phosphate-transferring domains form an asymmetric dimer in which the pseudokinase domain JH2 occupies the position of "receiver", while the kinase domain is the "activator" (Figure 5a). Upon cytokine receptor activation, the inhibitory JH1−JH2 conformation is displaced, and the domains are rearranged into an active state.[49] The JH1−JH2 model proposed in this study could be one dimer in a tetramer which is formed by four phosphate-transferring domains from two JAK2s. The existence of tetramers and even higher order oligomers has been demonstrated for EGFR[50] and other protein kinases.[51]

Our work explains the abolition of the JH2-mediated regulation of JAK2 by the activating mutation V617F. The interactions between the two domains in the asymmetric dimer (Figure 5a) preclude the JH1 domain from adopting an active conformation. The V617F mutation in JH2 relieves negative regulation by preventing JH1−JH2 association from the asymmetric form as shown in Figure 5a. After their separation, the JH1 and JH2 domains may rearrange to interact in other conformations, possibly including a JH1−JH1 homodimer (Figure 5b)[49] because of the favorable interaction between two JH1 domains.[48] The two domains could still be arranged in an asymmetric form, but one of the kinase domains JH1 takes the receiver position and adopts a conformation that fully activates JAK2 kinase (Figure 5b). Based on the JH1-JH2 model proposed in this study, the dual (both negative and positive) regulation of the JH2 domain[11] could be explained by the possible weakened/strengthened JH1-JH2 interaction induced by JH2 mutations, which makes the domains easier/harder to separate for conformational rearrangement. It will be important

to obtain X-ray crystallography structures of JH1−JH2 domains as these may help to establish whether JAK2 is regulated through the asymmetric dimer, as suggested by our study. Verification of the mechanism proposed here must await detailed structural and biochemical analyses.

AUTHOR INFORMATION

Corresponding Author

*Phone: +44 (0)20 7679 4850. Fax: +44 (0)20 7679 1501. E-mail: p.v.coveney@ucl.ac.uk.

Notes

The authors declare no competing financial interest.

ACKNOWLEDGMENTS

This research was supported by the EU FP7 ContraCancrum (ICT-2007.5.30) and p-medicine (ICT-2009.5.3) projects and partially supported by the DEISA Consortium (cofunded by the EU, FP7 project 222919) which provided access to HECToR, the UK's national supercomputer based in Edinburgh.

REFERENCES

(1) Imada, K.; Leonard, W. J. The Jak-STAT pathway. *Mol. Immunol.* **2000**, *37* (1−2), 1−11.

(2) Aaronson, D. S.; Horvath, C. M. A road map for those who don't know JAK-STAT. *Science* **2002**, *296* (5573), 1653−1655.

(3) Boudny, V.; Kovarik, J. JAK/STAT signaling pathways and cancer - minireview. *Neoplasma* **2002**, *49* (6), 349−355.

(4) Shuai, K.; Liu, B. Regulation of JAK-STAT signalling in the immune system. *Nat. Rev. Immunol.* **2003**, *3* (11), 900−911.

(5) Cohen, P. Protein kinases - the major drug targets of the twenty-first century? *Nat. Rev. Drug Discovery* **2002**, *1* (4), 309−315.

(6) Saharinen, P.; Silvennoinen, O. The pseudokinase domain is required for suppression of basal activity of Jak2 and Jak3 tyrosine kinases and for cytokine-inducible activation of signal transduction. *J. Biol. Chem.* **2002**, *277* (49), 47954−47963.

(7) Zeqiraj, E.; van Aalten, D. M. F. Pseudokinases-remnants of evolution or key allosteric regulators? *Curr. Opin. Struct. Biol.* **2010**, *20* (6), 772−781.

(8) Matthews, D. J.; Gerritsen, M. E. Appendix XIII tumor associated mutations in JAK2. In *Targeting Protein Kinases for Cancer Therapy*; John Wiley & Sons, Inc.: NJ, 2010.

(9) Lippert, E.; Boissinot, M.; Kralovics, R.; Girodon, F.; Dobo, I.; Praloran, V.; Boiret-Dupre, N.; Skoda, R. C.; Hermouet, S. The JAK2-V617F mutation is frequently present at diagnosis in patients with essential thrombocythemia and polycythemia vera. *Blood* **2006**, *108* (6), 1865−1867.

(10) Johnson, S. A.; Hunter, T. Kinomics: methods for deciphering the kinome. *Nat. Methods* **2005**, *2* (1), 17−25.

(11) Bandaranayake, R. M.; Ungureanu, D.; Shan, Y.; Shaw, D. E.; Silvennoinen, O.; Hubbard, S. R. Crystal structures of the JAK2 pseudokinase domain and the pathogenic mutant V617F. *Nat. Struct. Mol. Biol.* **2012**, *19* (8), 754−759.

(12) Lindauer, K.; Loerting, T.; Liedl, K. R.; Kroemer, R. T. Prediction of the structure of human Janus kinase 2 (JAK2) comprising the two carboxy-terminal domains reveals a mechanism for autoregulation. *Protein Eng.* **2001**, *14* (1), 27−37.

(13) Giordanetto, F.; Kroemer, R. T. Prediction of the structure of human Janus kinase 2 (JAK2) comprising JAK homology domains 1 through 7. *Protein Eng.* **2002**, *15* (9), 727−737.

(14) Maures, T. J.; Kurzer, J. H.; Carter-Su, C. SH2B1 (SH2-B) and JAK2: a multifunctional adaptor protein and kinase made for each other. *Trends Endocrinol. Metab.* **2007**, *18* (1), 38−45.

(15) Mohammadi, M.; Schlessinger, J.; Hubbard, S. R. Structure of the FGF receptor tyrosine kinase domain reveals a novel auto-inhibitory mechanism. *Cell* **1996**, *86* (4), 577−587.

(16) Dusa, A.; Mouton, C.; Pecquet, C.; Herman, M.; Constantinescu, S. N. JAK2 V617F constitutive activation requires JH2 residue F595: a pseudokinase domain target for specific inhibitors. *PLoS One* **2010**, *5* (6), e11157.

(17) Lee, T. S.; Ma, W. L.; Zhang, X.; Kantarjian, H.; Albitar, M. Structural effects of clinically observed mutations in JAK2 exons 13−15: comparison with V617F and exon 12 mutations. *BMC Struct. Biol.* **2009**, *9*, 58.

(18) Lee, T. S.; Ma, W. L.; Zhang, X.; Giles, F.; Kantarjian, H.; Albitar, M. Mechanisms of constitutive activation of janus kinase 2-V617F revealed at the atomic level through molecular dynamics simulations. *Cancer* **2009**, *115* (8), 1692−1700.

(19) Pellicena, P.; Kuriyan, J. Protein-protein interactions in the allosteric regulation of protein kinases. *Curr. Opin. Struct. Biol.* **2006**, *16* (6), 702−709.

(20) Zhang, X. W.; Gureasko, J.; Shen, K.; Cole, P. A.; Kuriyan, J. An allosteric mechanism for activation of the kinase domain of epidermal growth factor receptor. *Cell* **2006**, *125* (6), 1137−1149.

(21) Bae, J. H.; Boggon, T. J.; Tome, F.; Mandiyan, V.; Lax, I.; Schlessinger, J. Asymmetric receptor contact is required for tyrosine autophosphorylation of fibroblast growth factor receptor in living cells. *Proc. Natl. Acad. Sci. U.S.A.* **2010**, *107* (7), 2866−2871.

(22) Zhang, X. W.; Pickin, K. A.; Bose, R.; Jura, N.; Cole, P. A.; Kuriyan, J. Inhibition of the EGF receptor by binding of MIG6 to an activating kinase domain interface. *Nature* **2007**, *450* (7170), 741−744.

(23) Mi, L. Z.; Lu, C. F.; Li, Z. L.; Nishida, N.; Walz, T.; Springer, T. A. Simultaneous visualization of the extracellular and cytoplasmic domains of the epidermal growth factor receptor. *Nat. Struct. Mol. Biol.* **2011**, *18* (9), 984−989.

(24) Jura, N.; Shan, Y. B.; Cao, X. X.; Shaw, D. E.; Kuriyan, J. Structural analysis of the catalytically inactive kinase domain of the human EGF receptor 3. *Proc. Natl. Acad. Sci. U.S.A.* **2009**, *106* (51), 21608−21613.

(25) Jeffrey, P. D.; Ruso, A. A.; Polyak, K.; Gibbs, E.; Hurwitz, J.; Massague, J.; Pavletich, N. P. Mechanism of Cdk activation revealed by the structure of a Cyclina-Cdk2 complex. *Nature* **1995**, *376* (6538), 313−320.

(26) Neiditch, M. B.; Federle, M. J.; Pompeani, A. J.; Kelly, R. C.; Swem, D. L.; Jeffrey, P. D.; Bassler, B. L.; Hughson, F. M. Ligand-induced asymmetry in histidine sensor kinase complex regulates quorum sensing. *Cell* **2006**, *126* (6), 1095−1108.

(27) Bae, J. H.; Schlessinger, J. Asymmetric tyrosine kinase arrangements in activation or autophosphorylation of receptor tyrosine kinases. *Mol. Cells* **2010**, *29* (5), 443−448.

(28) Macdonald-Obermann, J. L.; Piwnica-Worms, D.; Pike, L. J. Mechanics of EGF receptor/ErbB2 kinase activation revealed by luciferase fragment complementation imaging. *Proc. Natl. Acad. Sci. U.S.A.* **2012**, *109* (1), 137−142.

(29) Fiser, A.; Sali, A. MODELLER: Generation and refinement of homology-based protein structure models. *Macromolecular Crystallography, Part D* **2003**, *374*, 461−491.

(30) Stamos, J.; Sliwkowski, M. X.; Eigenbrot, C. Structure of the epidermal growth factor receptor kinase domain alone and in complex with a 4-anilinoquinazoline inhibitor. *J. Biol. Chem.* **2002**, *277* (48), 46265−46272.

(31) Antonysamy, S.; Hirst, G.; Park, F.; Sprengeler, P.; Stappenbeck, F.; Steensma, R.; Wilson, M.; Wong, M. Fragment-based discovery of JAK-2 inhibitors. *Bioorg. Med. Chem. Lett.* **2009**, *19* (1), 279−282.

(32) Sadiq, S. K.; Wright, D.; Watson, S. J.; Zasada, S. J.; Stoica, I.; Coveney, P. V. Automated molecular simulation based binding affinity calculator for ligand-bound HIV-1 proteases. *J. Chem. Inf. Model.* **2008**, *48* (9), 1909−1919.

(33) Jorgensen, W. L.; Chandrasekhar, J.; Madura, J. D.; Impey, R. W.; Klein, M. L. Comparison of simple potential functions for simulating liquid water. *J. Chem. Phys.* **1983**, *79* (2), 926−935.

(34) Duan, Y.; Wu, C.; Chowdhury, S.; Lee, M. C.; Xiong, G. M.; Zhang, W.; Yang, R.; Cieplak, P.; Luo, R.; Lee, T.; Caldwell, J.; Wang, J. M.; Kollman, P. A point-charge force field for molecular mechanics

simulations of proteins based on condensed-phase quantum mechanical calculations. *J. Comput. Chem.* **2003**, *24* (16), 1999−2012.
(35) Phillips, J. C.; Braun, R.; Wang, W.; Gumbart, J.; Tajkhorshid, E.; Villa, E.; Chipot, C.; Skeel, R. D.; Kale, L.; Schulten, K. Scalable molecular dynamics with NAMD. *J. Comput. Chem.* **2005**, *26* (16), 1781−1802.
(36) Srinivasan, J.; Cheatham, T. E.; Cieplak, P.; Kollman, P. A.; Case, D. A. Continuum solvent studies of the stability of DNA, RNA, and phosphoramidate - DNA helices. *J. Am. Chem. Soc.* **1998**, *120* (37), 9401−9409.
(37) Case, D. A.; Cheatham, T. E.; Darden, T.; Gohlke, H.; Luo, R.; Merz, K. M.; Onufriev, A.; Simmerling, C.; Wang, B.; Woods, R. J. The Amber biomolecular simulation programs. *J. Comput. Chem.* **2005**, *26* (16), 1668−1688.
(38) Dixit, A.; Verkhivker, G. M. Hierarchical modeling of activation mechanisms in the ABL and EGFR kinase domains: thermodynamic and mechanistic catalysts of kinase activation by cancer mutations. *PLoS Comput. Biol.* **2009**, *5* (8), e1000487.
(39) Scott, L. M. The JAK2 exon 12 mutations: a comprehensive review. *Am. J. Hematol.* **2011**, *86* (8), 668−676.
(40) Krieger, E.; Joo, K.; Lee, J.; Lee, J.; Raman, S.; Thompson, J.; Tyka, M.; Baker, D.; Karplus, K. Improving physical realism, stereochemistry, and side-chain accuracy in homology modeling: Four approaches that performed well in CASP8. *Proteins: Struct., Funct., Bioinf.* **2009**, *77*, 114−122.
(41) Zhou, H. X. Association and dissociation kinetics of colicin E3 and immunity protein 3: convergence of theory and experiment. *Protein Sci.* **2003**, *12* (10), 2379−2382.
(42) Wan, S.; Coveney, P. V. Rapid and accurate ranking of binding affinities of epidermal growth factor receptor sequences with selected lung cancer drugs. *J. R. Soc. Interface* **2011**, *8*, 1114−1127.
(43) Dusa, A.; Staerk, J.; Elliott, J.; Pecquet, C.; Poirel, H. A.; Johnston, J. A.; Constantinescu, S. N. Substitution of pseudokinase domain residue Val-617 by large non-polar amino acids causes activation of JAK2. *J. Biol. Chem.* **2008**, *283* (19), 12941−12948.
(44) Mead, A. J.; Rugless, M. J.; Jacobsen, S. E. W.; Schuh, A. Germline JAK2 mutation in a family with hereditary thrombocytosis. *N. Engl. J. Med.* **2012**, *366* (10), 967−969.
(45) Gordon, G. M.; Lambert, Q. T.; Daniel, K. G.; Reuther, G. W. Transforming JAK1 mutations exhibit differential signalling, FERM domain requirements and growth responses to interferon-gamma. *Biochem. J.* **2010**, *432*, 255−265.
(46) Jura, N.; Endres, N. F.; Engel, K.; Deindl, S.; Das, R.; Lamers, M. H.; Wemmer, D. E.; Zhang, X. W.; Kuriyan, J. Mechanism for activation of the EGF receptor catalytic domain by the juxtamembrane segment. *Cell* **2009**, *137* (7), 1293−1307.
(47) Butcher, C. M.; Hahn, U.; To, L. B.; Gecz, J.; Wilkins, E. J.; Scott, H. S.; Bardy, P. G.; D'Andrea, R. J. Two novel JAK2 exon 12 mutations in JAK2V617F-negative polycythaemia vera patients. *Leukemia* **2008**, *22* (4), 870−873.
(48) Saharinen, P.; Takaluoma, K.; Silvennoinen, O. Regulation of the Jak2 tyrosine kinase by its pseudokinase domain. *Mol. Cell. Biol.* **2000**, *20* (10), 3387−3395.
(49) Saharinen, P.; Vihinen, M.; Silvennoinen, I. Autoinhibition of Jak2 tyrosine kinase is dependent on specific regions in its pseudokinase domain. *Mol. Biol. Cell* **2003**, *14* (4), 1448−1459.
(50) Clayton, A. H. A.; Walker, F.; Orchard, S. G.; Henderson, C.; Fuchs, D.; Rothacker, J.; Nice, E. C.; Burgess, A. W. Ligand-induced dimer-tetramer transition during the activation of the cell surface epidermal growth factor receptor-A multidimensional microscopy analysis. *J. Biol. Chem.* **2005**, *280* (34), 30392−30399.
(51) Lemmon, M. A.; Schlessinger, J. Cell signaling by receptor tyrosine kinases. *Cell* **2010**, *141* (7), 1117−1134.
(52) Wan, S. Z.; Stote, R. H.; Karplus, M. Calculation of the aqueous solvation energy and entropy, as well as free energy, of simple polar solutes. *J. Chem. Phys.* **2004**, *121* (19), 9539−9548.